JACS
JOURNAL OF THE AMERICAN CHEMICAL SOCIETY

ARTICLE

pubs.acs.org/JACS

Factors Controlling the Reactivity of Zinc Finger Cores

Yu-Ming Lee[†,‡] and Carmay Lim*[,†,‡]

[†]Department of Chemistry, National Tsing Hua University, Hsinchu 300, Taiwan

[‡]Institute of Biomedical Sciences, Academia Sinica, Taipei 115, Taiwan

Supporting Information

ABSTRACT: Although the Zn^{2+} cation in $Zn{\cdot}Cys_4$, $Zn{\cdot}Cys_3His$, $Zn{\cdot}Cys_2His_2$, and Zn_2Cys_6 cores of zinc finger (Zf) proteins typically plays a structural role, the Zn-bound thiolates in some Zf cores are reactive. Such labile Zf cores can serve as drug targets for retroviral or cancer therapies. Previous studies showed that the reactivity of a Zn-bound thiolate toward electrophiles is significantly reduced if it forms S---NH hydrogen bonds with the backbone amide. However, we found several well-known inactive Zf cores containing Cys ligands with no H-bonding interactions. Here, we show that H bonds from the peptide backbone or bonds from a second Zn cation to Zn-bound S atoms suppress the reactivity not only of these S atoms, but also of Zn-bound S* atoms with no interactions. Indeed, two or more indirect NH---S hydrogen bonds raise the free energy barrier for methylation of a Zn-bound S* in a Cys_4 core more than a direct NH---S* hydrogen bond. These findings help to elucidate why several well-known Zf cores have Cys ligands with no H bonds, but are unreactive. They also help to provide guidelines for distinguishing labile Cys-rich Zn sites from structural ones, which in turn help to identify novel potential Zf drug targets.

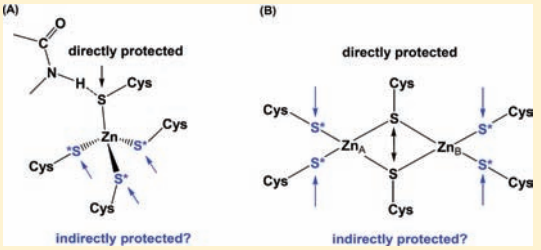

INTRODUCTION

Two or more cysteines are usually found in Zn-binding sites that are mainly involved in protein structure stabilization as opposed to catalysis.[1−7] Such structural Zn-sites are commonly found in zinc finger (Zf) proteins that contain one or two Zn^{2+} tetrahedrally coordinated to ≥2 cysteines and ≤2 histidines, forming four major kinds of cores: $Zn{\cdot}Cys_4$, $Zn{\cdot}Cys_3His$, $Zn{\cdot}Cys_2His_2$, and Zn_2Cys_6. The Zn^{2+} in Zf's plays a structural role: it induces the correct folding of Zf peptides, stabilizing the local protein structure that is required for function. Thus, Zf's are small protein domains stabilized by one or more structural Zn^{2+} cations. They typically function as interaction modules, and by binding DNA, RNA, proteins, or small molecules, they are involved in many fundamental cellular processes such as replication and repair, transcription and translation, cell proliferation and apoptosis, metabolism, and signaling.[7,8]

Our previous work provided a physical basis for why ≥2 Cys^- are often found in structural Zn sites but are rarely found in catalytic sites where Zn^{2+} can act as a Lewis acid (electron-pair acceptor):[9] Most structural Zn sites are Cys-rich with a coordination number of 4, as Cys^- transfers more charge to Zn^{2+} than do the other amino acid and water ligands,[10,11] thereby reducing the metal's positive charge and electron-accepting ability. Furthermore, steric repulsion among the bulky $Cys(S^-)$ inhibits Zn^{2+} from binding a fifth ligand. Hence, charge transfer and steric effects of ≥2 Cys^- ligands prevent the Zn^{2+} from serving as a Lewis acid in catalysis. These principles also help to explain why no natural Zf domains with His_4 or His_3Cys cores exist: if Zn^{2+} were to bind to one or no Cys^-, it could act as a Lewis acid and bind another ligand.[9]

Although Zf cores typically play a structural role, some Zf cores can be chemically activated and can serve as drug targets for retroviral or cancer therapies.[12] Such Zf cores are referred to as labile herein because the Zn-bound thiolate is reactive, whereas Zn^{2+} still plays a structural role. The Zn-bound S atoms can undergo reversible/irreversible oxidation, accompanied by Zn release, which in turn alters protein function.[7] For example, the Zn-bound S atoms of the Cys_3His core in the HIV-1 nucleocapsid p7 protein can be oxidized by Zn-ejecting reagents such as disulfide benzamide, resulting in Zn^{2+} ejection and loss of viral protein structure and function,[13−16] but they do not affect cellular human Zf functions.[17] Disulfide benzamide and benzisothiazolone derivatives can also successfully eject Zn^{2+} from the Zf cores of human estrogen receptor DNA-binding domain; hence, they have been employed in the development of an alternative therapy for breast cancer.[18,19] Apart from Zf cores, the $Zn{\cdot}Cys_4$ site in the N-terminal domain of the *E. coli* Ada protein (N-Ada), which plays a role in methylated DNA damage repair, is also reactive. It promotes the transfer of a methyl group from the methylated DNA to a specific Zn ligand, Cys38. Interestingly, the other three Zn-bound cysteines of N-Ada do not react with the methyl group.[20]

For a given Zn-site, what factors determine whether a Zn-bound thiolate is inert or reactive? Both experimental[21] and theoretical[22−24] studies show that the net charge of the Zn core affects the nucleophilicity of the Zn-bound thiolate: a more negatively charged Zf core will tend to increase the inherent reactivity of a Zn-bound thiolate than will a neutral one.

Received: March 9, 2011
Published: May 16, 2011

dx.doi.org/10.1021/ja202165x | J. Am. Chem. Soc. 2011, 133, 8691–8703

Table 1. Zf Cores Containing Cys Ligands with No H Bonds and Their Solvent-Accessible Surface Area (SASA)

PDB entry	protein name	cysteines with no H bonds[a,b]	SASA (%)[c]	cysteines with H bonds[a,d]
		Structural Zn Sites		
	$Zn\cdot Cys_4$ sites			
1lat	glucocorticoid receptor	C^{440}, C^{457}	1	C^{443}(bb), C^{460}(sc^+)
1u8b	Ada·DNA complex	C^{38}, C^{42}	8	C^{69}(bb), C^{72}(bb)
2jvn	Human PARP-1	C^{298}, C^{321}	8	C^{295}S(bb), C^{311}(bb)
1het	alcohol dehydrogenase	C^{103}	10	C^{97}(bb), C^{100}(bb), C^{111}(bb)
	$Zn\cdot Cys_3His$ sites			
1dsv	MMTV-1 NCp10 ZD2	C^{58}, C^{61}, C^{71}	9	none
2exf	HIV-1 NCp7 ZD1	C^{15}, C^{18}, C^{28}	20	none
1pud	tRNA-guanine transglycosylase	C^{320}, C^{323}	4	C^{318}(bb and sc)
1a74	I-ppol homing endonuclease	C^{41}, C^{100}	2	C^{105}(bb)
1ptq	protein kinase C delta	C^{272}	15	C^{244}(bb), C^{247}(bb)
	$Zn\cdot Cys_2His_2$ sites			
1aay	Zif268	C^{107}, C^{112}	16	none
1clc	endoglucanase d	C^{155}, C^{173}	2	none
1tf3	Zf of TFIIIA	C^{15}	26	C^{50}(sc^+)
	Zn_2Cys_6 sites			
1zme	PUT3—DNA complex	C^{34}, C^{37}, C^{50} C^{53}, C^{60}	3	C^{44}(sc)
1pyi	PPR1—DNA complex	C^{34}, C^{37}, C^{44} C^{51}, C^{54}	2	C^{61}(bb)
		Labile Zn Sites		
	$Zn\cdot Cys_4$ sites			
1hcp	Human/chicken estrogen receptor	C^{43}, C^{49}, C^{59}, C^{62}	19	none
1eyf	Ada protein (free form)	C^{38}, C^{42}, C^{69}, C^{72}	8	none
	$Zn\cdot Cys_3His$ sites			
1fu9	FOG-1	C^{11}, C^{14}, C^{32}	11	none
1dsq	MMTV-1 NCp10 ZD1	C^{31}, C^{34}, C^{44}	27	none
2exf	HIV-1 NCp7 ZD2	C^{36}, C^{39}, C^{49}	17	none
2oq6	histone demethylase JMJD2A	C^{234}, C^{306}, C^{308}	19	none

[a] Hydrogen bonds to the Zn-bound cysteines were computed using HBPLUS.[32] [b] Unsheltered cysteines with no H bonds to other amino acid residues in the Zf; H bonds to water molecules were not counted. [c] The mean % SASA of the Zn-site was computed using NACCESS.[33] [d] The Zn-bound Cys forms H bonds to the backbone NH (bb) or a neutral side chain (sc) or a positively charged side chain (sc^+).

A statistical analysis of 207 Zf's from 92 protein structures showed that the degree of screening of the Zn-bound thiolates via backbone NH---S hydrogen bonds determines the reactivity of the Zn-bound thiolate.[25] Thus, the reactive $Zn\cdot Cys_4$ core of N-Ada was found to be less electrostatically screened via H bonds than the unreactive Cys_4 cores of GATA Zf's. Subsequent experimental[26−28] and theoretical[23] studies on model complexes of Zn metalloproteins confirm that a single H bond between an amide N−H and a Zn−bound thiolate can significantly reduce its reactivity toward electrophiles. Furthermore, although in the NMR[29] structure of free N-Ada, the Zn-bound cysteines exhibit no H bonds, in the X-ray[20] structure of methylated N-Ada complexed with DNA, backbone NH---S hydrogen bonds are absent at the uniquely reactive Cys38, but are present at the other unreactive cysteines.[30] Altogether, these findings suggest that NH---S hydrogen bonds can suppress the Zn-bound thiolate reactivity.

The above H-bond protection argument, which is used to explain the exclusive reactivity of Cys38 in N-Ada,[12] implies that for a Cys-rich Zn core to be inert, each Zn-bound thiolate needs to be masked by one or more H bonds to suppress its reactivity.

Scheme 1. (A) Can a Direct H Bond from the Peptide Backbone to Cys S Suppress the Reactivity Not Only of S, but Also the Other Zn-Bound S*; and (B) Can Bonds from a Second Zn Cation to the Bridging S Atoms Suppress the Reactivity of the Terminal Zn-Bound S*?

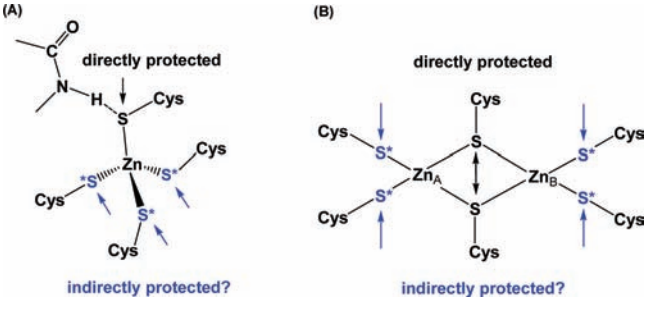

However, when we surveyed X-ray and NMR structures of Zf cores in the Protein Data Bank (PDB),[31] several well-known inert Zf cores

dx.doi.org/10.1021/ja202165x | J. Am. Chem. Soc. 2011, 133, 8691–8703

Scheme 2. Schematic Diagram Showing Two Possible Pathways for *E. coli* N-Ada Reacting with Methylated DNA

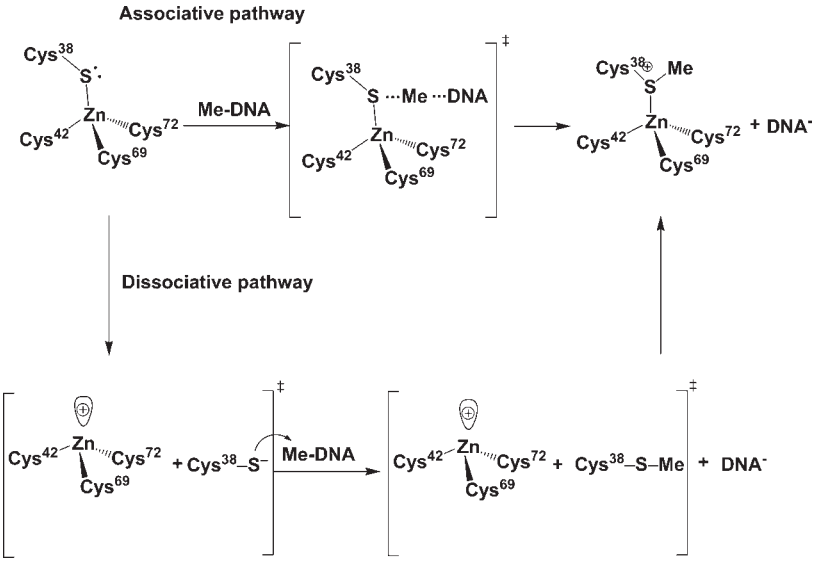

Scheme 3

$$\begin{array}{ccc} & \Delta G^{I} & \\ A\ (\varepsilon = 1) & \rightarrow & B\ (\varepsilon = 1) \\ \Delta G_{solv}{}^{x}\ (A) \downarrow & & \downarrow \Delta G_{solv}{}^{x}\ (B) \\ A\ (\varepsilon = x) & \rightarrow & B\ (\varepsilon = x) \\ & \Delta G^{x} & \end{array}$$

possess unsheltered Cys ligands with no H-bonding interactions (see Table 1). Notably, the Zn·Cys_4 site of alcohol dehydrogenase (1het) contains a Cys with no H bonds to other amino acid residues like Cys 38 in N-Ada, while the Zn·Cys_4 sites of human PARP-1 (2jvn) and glucocorticoid receptor each contains two unsheltered cysteines. Hence, the H-bond protection argument does not explain why N-Ada is uniquely active as compared to structural Zf's containing the same Zn·Cys_4 motif. Furthermore, some Zf's containing polynuclear Zn-sites exhibit a lack of H-bond protection. For example, the Zn_2Cys_6 cores in PUT3 (1zme) and PPR1 (1pyi) proteins complexed with DNA each has only a single H bond to second-shell residues, while the other five cysteines are unsheltered.

The results in Table 1 suggest that additional factors are involved in protecting structural Zf cores from unwanted reactions. We hypothesize that unsheltered Cys ligands may be protected by indirect interactions with other cysteines, as illustrated in Scheme 1. Thus, this work aims to answer the following questions: (1) Can indirect H bonds to Cys ligands stabilize the Zf core and inhibit reaction at the other unsheltered Cys ligands (Scheme 1A)? (2) Can bonds from a second Zn cation to the bridging S atoms stabilize the binuclear Zf core and inhibit reaction at the terminal cysteines? (3) How does solvent exposure of the Zf core affect its reactivity?

To address the above questions, we chose the *E. coli* N-Ada domain as a model system because experimental data are available to set up and validate the calculations. Transfer of the methyl group from the methylated DNA to the Zn-bound Cys may proceed via a dissociative or an associative pathway (see Scheme 2).[28,34,35]

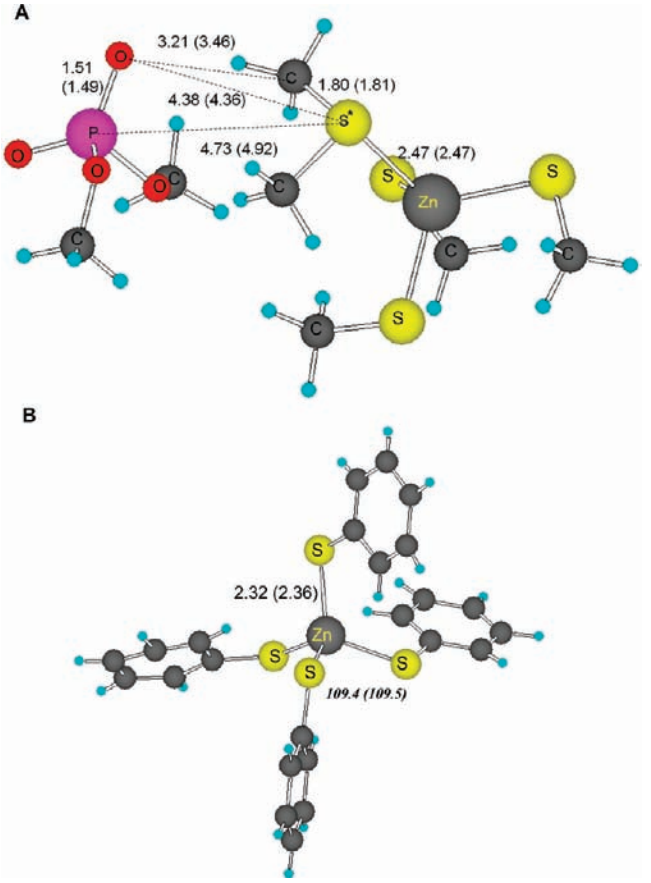

Figure 1. Comparison between fully optimized S-VWN/6-31+G(d) and X-ray geometries of (A) $[Zn(MeS)_4Me]\cdots(MeO)_2PO_2$ and (B) Zn·$(SPh)_4$. Numbers without parentheses correspond to calculated distances (in Å) and angles (in deg), whereas numbers in parentheses are the respective values in the X-ray structure, PDB entry 1u8b for (A) and CSD entry GAKKUY for (B).

The dissociative pathway[21,36,37] involves two steps: first, the nucleophile, Cys38, dissociates from the Zn·Cys_4 core; second,

dx.doi.org/10.1021/ja202165x |J. Am. Chem. Soc. 2011, 133, 8691–8703

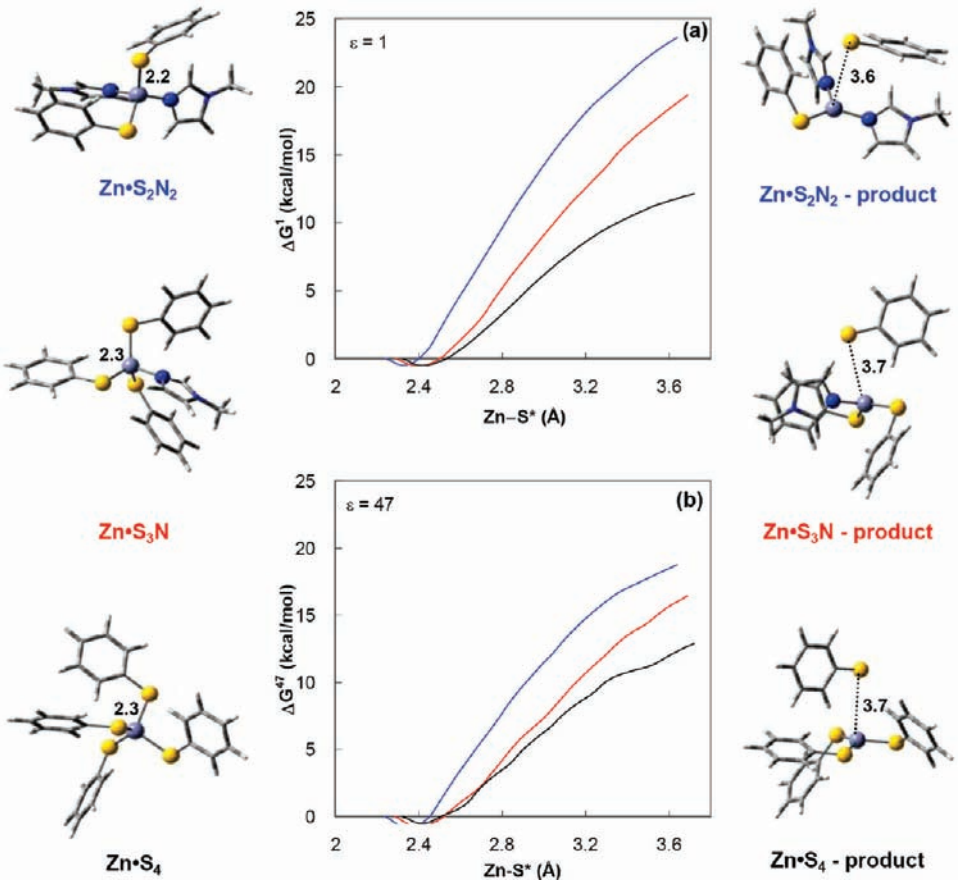

Figure 2. Free energy (in kcal/mol) as a function of the distance between Zn and the departing S* in $[Zn(SC_6H_5)_2(MeIm)_2]^0$ ($Zn \cdot S_2N_2$, blue curve), $[Zn(SC_6H_5)_3(MeIm)]^-$ ($Zn \cdot S_3N$, red curve), and $[Zn(SC_6H_5)_4]^{2-}$ ($Zn \cdot S_4$, black curve) in (a) the gas phase ($\varepsilon = 1$) and (b) DMSO ($\varepsilon = 47$). The fully optimized S-VWN/6-31+G(d) geometries of the Zn complexes are depicted on the left, while the respective constrained optimized structures with the Zn−S* distances fixed at 3.6 or 3.7 Å are shown on the right.

the free thiolate attacks the methyl group on the substrate (methylated DNA) and subsequently rebinds the Zn. The associative pathway[26,38,39] involves a single step where the methylated DNA methyl group is transferred to the Zn-bound Cys38. Because it is not clear if the reaction proceeds via a dissociative or associative pathway,[21,26,28,34,35,37,38] we computed the key steps in both pathways for each model Zn complex: (1) the transfer of a methyl group to a Zn-bound thiolate in the associative pathway,[38,39] and (2) initial dissociation of a Zn-bound thiolate, assumed to be rate-limiting in the dissociative pathway.[21,36,37] On the basis of the results obtained, we derived guidelines for distinguishing labile Zf cores from structural ones.

METHODS

Models Used. The reaction modeled is transfer of a CH_3^+ group from methylated DNA to a Zn-bound Cys in a Zf core via an associative or a dissociative pathway. The Zn ligands, Cys and His, were modeled by methyl thiolate (CH_3S^-) and imidazole, respectively. Our previous work[40] showed that the most common second-shell interaction partner for the Zn-bound Cys is the backbone peptide group, which was modeled by $CH_3CONHCH_3$. In model Cys_3His and Cys_2His_2 Zf cores, however, the free NH of imidazole can form an unwanted H bond with the CO group of $CH_3CONHCH_3$, which would affect the chemical properties of these Zf cores.[41,42] As our aim is to evaluate the effect of a NH---S hydrogen bond on the reactivity of an unprotected Cys, and a H bond between a Zn-bound Cys at position *i* and the backbone amide at position *i*+2 is commonly found in 3D structures (e.g., in PDB entries 1alt, 1anv, 1faq, 1bbo, 1ncs), we used $-(CH_2)_5(CONH)CH_3$ as the backbone model for Cys_3His and Cys_2His_2 Zf cores.

Geometry Optimization. In previous studies,[41,43] the S-VWN functional and the 6-31+G(d) basis set have been shown to be adequate for reproducing metal−ligand bond distances in several Zn complexes within experimental error. Consequently, full geometry optimization for all of the reactant/product complexes was carried out using the Gaussian 03[44] program at the S-VWN/6-31+G(d) level. For each fully optimized structure, S-VWN/6-31+G(d) vibrational frequencies were then computed to verify that the reactant/product complex was at the minimum of its potential energy surface. No imaginary frequency was found in any of the fully optimized reactant/product complex geometries.

In modeling the first step of the dissociation pathway, the reaction coordinate was chosen to be the distance between the Zn and the departing S*, which was elongated from its optimized bond distance to 3.7 Å in 0.1 Å increments. On the other hand, in modeling the association pathway, the reaction coordinate was chosen to be the distance between the attacking Zn-bound S* and the closest carbon of $(MeO)_3PO$, which was reduced from its optimized value to 1.8 Å at 0.1 Å intervals. The geometry for a fixed reaction coordinate was optimized and used to compute the energy profiles.

Gas-Phase Free Energy Calculations. On the basis of the fully/constrained optimized S-VWN/6-31+G(d) geometries,

dx.doi.org/10.1021/ja202165x |*J. Am. Chem. Soc.* 2011, 133, 8691–8703

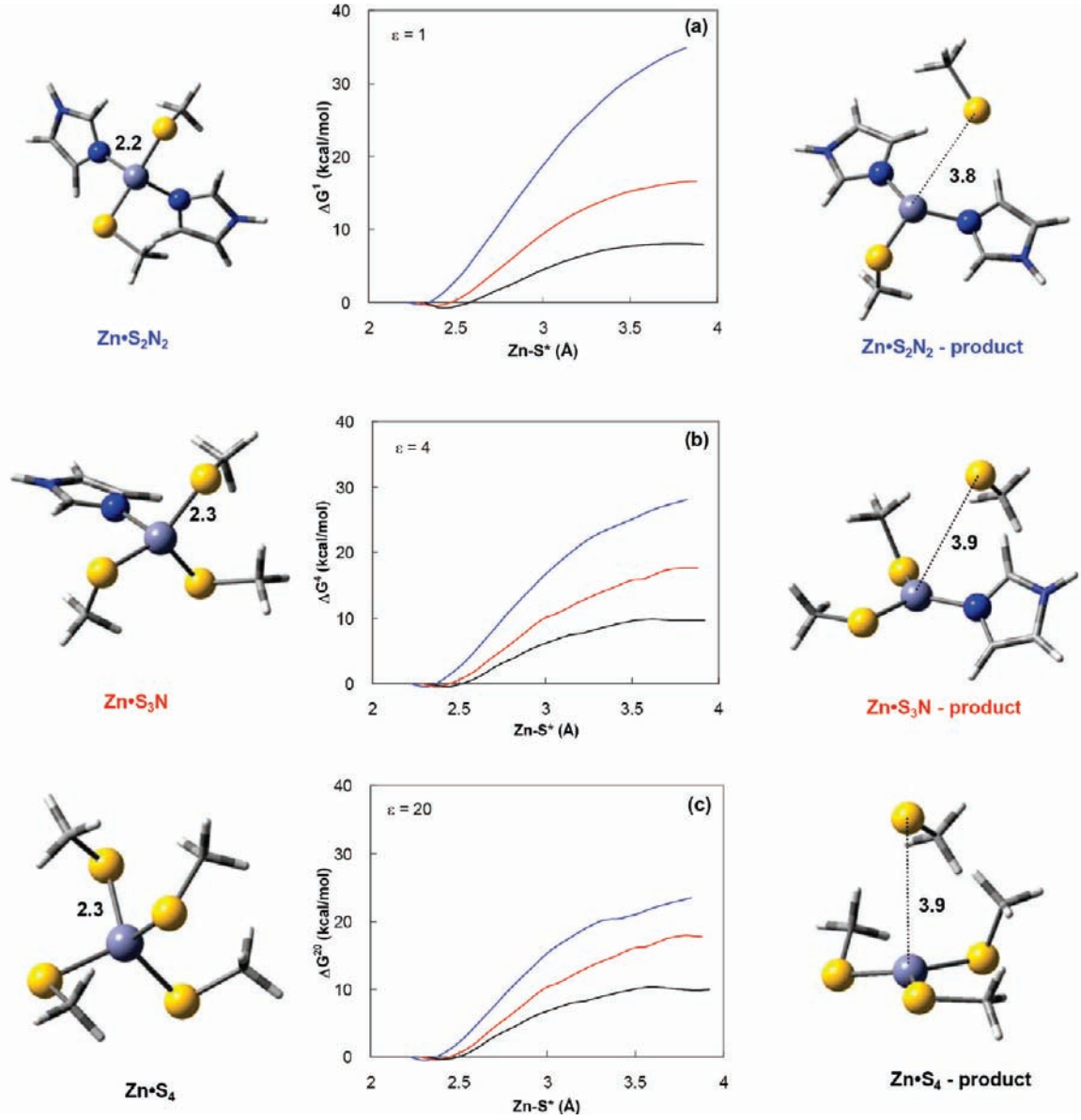

Figure 3. Free energy (in kcal/mol) as a function of the distance between Zn and the departing S* in $[Zn(MeS)_2(Im)_2]^0$ ($Zn \cdot S_2N_2$, blue curve), $[Zn(MeS)_3(Im)]^-$ ($Zn \cdot S_3N$, red curve), and $[Zn(MeS)_4]^{2-}$ ($Zn \cdot S_4$, black curve) in (a) the gas phase ($\varepsilon = 1$), (b) buried sites ($\varepsilon = 4$), and (c) partially buried sites ($\varepsilon = 20$). The fully optimized S-VWN/6-31+G(d) geometries of the isolated metal complexes are depicted on the left, while the respective constrained optimized structures with the Zn−S* distances fixed at 3.8 or 3.9 Å are shown on the right.

B3LYP/6-311++G(2d,2p) was used to evaluate the electronic energies, E_{elec}, because this method has been shown to reproduce the experimental gas-phase deprotonation free energies of H_2S and has also been successfully used in metal-induced Zf folding calculations.[45] In computing the free energy difference between reactants and products, the vibrational frequencies were scaled by an empirical factor of 0.9833,[46] and the thermal energy including zero point energy (E_T), work (PV), and entropy (S) were evaluated using standard statistical mechanical formulas.[47] The differences in ΔE_{elec}, ΔE_T, ΔPV, and ΔS between the products and reactants were used to compute the gas-phase reaction free energy, ΔG^1, at room temperature (298 K) according to:

$$\Delta G^1 = \Delta E_{elec} + \Delta E_T + \Delta PV - T\Delta S \quad (1)$$

In computing the energy profiles for the dissociation or association pathway, the E_{elec} of the complex for a fixed reaction coordinate relative to that of the respective fully optimized complex (ΔE^1) was evaluated. Because the activation entropy ($T\Delta S^{\ddagger} = 0.07$ kcal/mol) for methylation of a thiolate bound to $Zn \cdot Cys_4$ was found to be negligible as compared to the respective activation energy (8.6 kcal/mol), the entropic changes were not included in the energy profiles; that is, $\Delta G^1 \approx \Delta E_{elec}$. At the peak of the energy profile for the association pathway, the geometry of the transition state (TS) was fully optimized. Each optimized TS was verified by a single imaginary frequency corresponding to the atomic displacement of the bond-forming and bond-breaking entities.

Solvation Free Energy Calculations. Because Zf cores in X-ray structures are relatively buried with SASA < 30% (Table 1),[25] its environment was characterized by a dielectric constant ε ranging from 4 (fully buried) to 20 (partially buried). The free energy, ΔG^x, was calculated according to Scheme 3, where ΔG^1 is the gas-phase free energy and ΔG_{solv}^x is the free energy for transferring a molecule from the

dx.doi.org/10.1021/ja202165x | J. Am. Chem. Soc. 2011, 133, 8691–8703

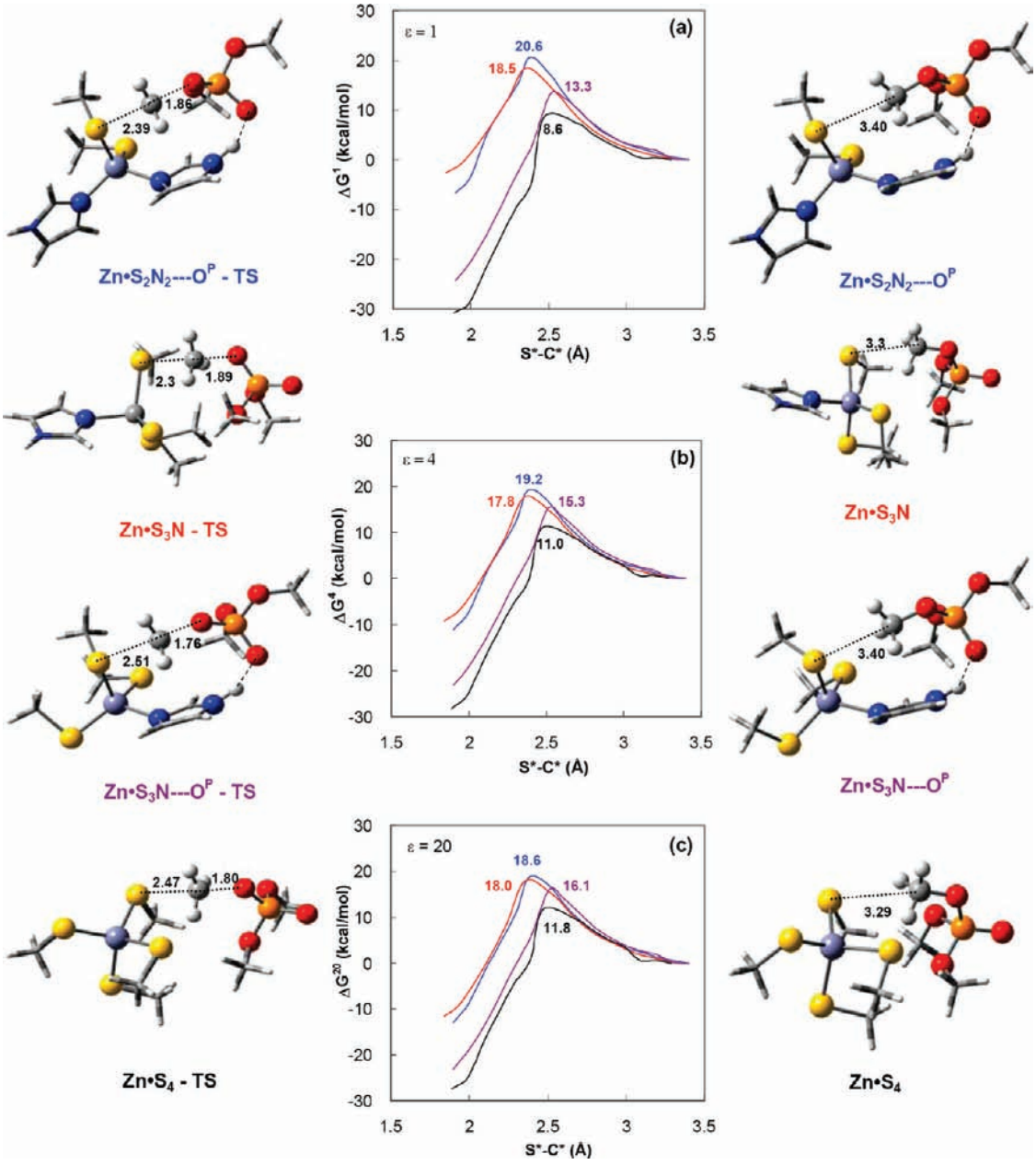

Figure 4. Free energy (in kcal/mol) as a function of the distance between the attacking S* and the closest carbon of $(MeO)_3PO$ in $[Zn(MeS)_2(Im)_2]^0$ ($Zn \cdot S_2N_2$---O^P, blue curve), $[Zn(MeS)_3(Im)]^-$ ($Zn \cdot S_3N$, red curve), $[Zn(MeS)_3(Im)]^-$ with a H bond between the imidazole NH and the phosphate O^P ($Zn \cdot S_3N$---O^P, violet curve), and $[Zn(MeS)_4]^{2-}$ ($Zn \cdot S_4$, black curve) in (a) the gas phase ($\varepsilon = 1$), (b) buried sites ($\varepsilon = 4$), and (c) partially buried sites ($\varepsilon = 20$). The fully optimized S-VWN/6-31+G(d) geometries of the reactants and transition states are depicted on the right and left, respectively. Dashed lines denote H bonds.

gas phase to a continuous medium characterized by dielectric constant, x. Thus, the ΔG^x can be computed from

$$\Delta G^x = \Delta G^1 + \Delta G^x_{solv}(B) - \Delta G^x_{solv}(A) \quad (2)$$

The solvation free energies were evaluated using the MEAD program,[48] as described in previous works.[43,49] Effective solute radii were obtained by adjusting the CHARMM version 22[50] van der Waals radii to reproduce the experimental hydration free energies of Zn^{2+} and model ligand molecules to within 1 kcal/mol (see Supporting Information, Table S1). They are as follows (in Å): $R_{Zn} = 1.40$, $R_H = 1.468$, R_H (PO_4) = 1.0, $R_C = 1.88$, $R_N = 1.80$, $R_O = 1.83$, $R_P = 2.10$, $R_S = 2.19$.

RESULTS

Validation of the Computed Geometries. Although our previous studies[5,11,41,43] had shown that the S-VWN/6-31+G(d) method could reproduce the geometries of complexes between Zn^{2+} and S-/N-containing ligands, we further validate this method by searching the PDB[31] and the Cambridge Structural Database[51] for X-ray structures similar to the Zn complexes studied. This yielded two relevant structures: (1) $[Zn(Cys)_4Me]\cdots(MeO)_2PO_2$ in the cocrystal structure of the N-Ada/DNA complex (PDB entry 1u8b) where the methyl group is attached to Cys38(S*) and (2) $[Zn \cdot (SPh)_4]^{2-}$ (CSD entry GAKKUY).

dx.doi.org/10.1021/ja202165x |J. Am. Chem. Soc. 2011, 133, 8691–8703

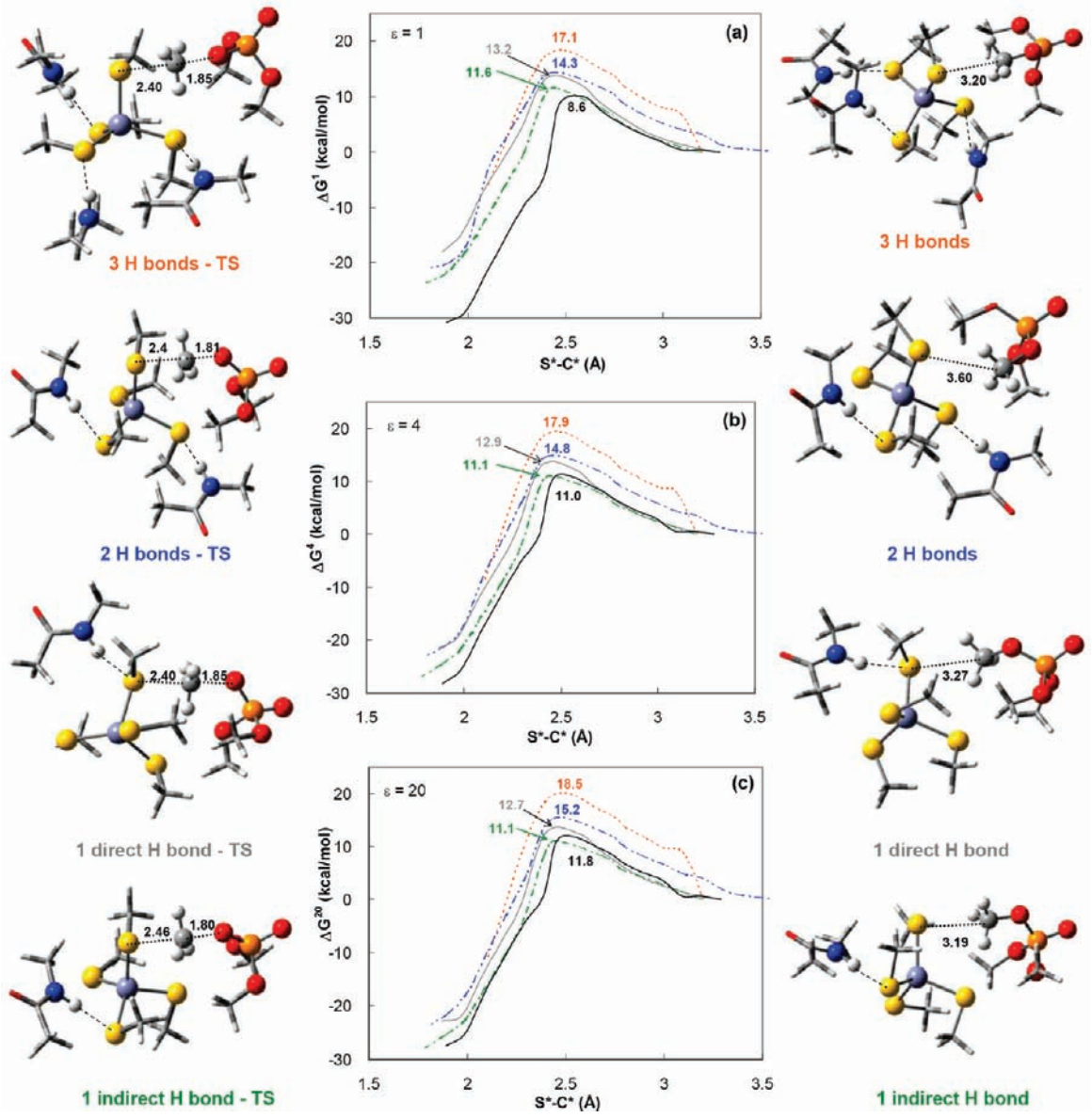

Figure 5. Free energy (in kcal/mol) as a function of the distance between the attacking S* and the closest carbon of $(MeO)_3PO$ in the $[Zn(MeS)_4]^{2-}$ complex with 1 (green curves), 2 (blue curves), and 3 (orange curves) indirect NH---S interactions in (a) the gas phase ($\varepsilon = 1$), (b) buried sites ($\varepsilon = 4$), and (c) partially buried sites ($\varepsilon = 20$). These free energy profiles are compared to those in the $[Zn(MeS)_4]^{2-}$ complex with no H bonds (black curves) and with a H bond to the reacting S atom (gray curves). The fully optimized S-VWN/6-31+G(d) geometries of the reactants and transition states are depicted on the right and left, respectively. Dashed lines denote H bonds.

Comparison of the S-VWN/6-31+G(d) optimized geometries with the corresponding X-ray structures shows good agreement. In the optimized $[Zn\cdot(MeS)_3Me_2S\cdots(MeO)_2PO_2]^{2-}$ complex (Figure 1a), the three thiolate ligands have similar bond distances (2.27−2.29 Å) that overlap with the respective X-ray distances (2.18−2.29 Å), whereas the thioether ligand has an elongated bond distance (2.47 Å) that is identical to the X-ray value, while the S*−CH_3 (1.80 Å), P−O (1.51 Å), and O−S* (4.38 Å) distances agree with the respective X-ray values to within 0.02 Å. Although the nonbonded O−C(S*) (3.21 Å) and P−S* (4.73 Å) distances underestimate the respective X-ray values by up to 0.25 Å, such errors are within experimental error, as X-ray distances of the same protein solved in different space groups (e.g., human carbonic anhydrase) differ by up to 0.40 Å. In the optimized $[Zn\cdot(SPh)_4]^{2-}$ complex (Figure 1b), the mean Zn−S distance (2.32 Å) and S−Zn−S (109.4°) angle agree with the respective X-ray values (CSD entry GAKKUY) to within 0.04 Å and 0.1°. Using increasingly larger basis sets (6-311++G(d,p), 6-311++G(2d,2p), and 6-311++G(2df,2p)) with the S-VWN functional does not significantly improve agreement with the X-ray values (see Supporting Information, Table S2). Using the same series of basis sets with the B3-LYP instead of the S-VWN functional yields a Zn−S distance (2.42 Å) in poorer agreement with the experimental value (2.36 ± 0.02 Å). As the focus herein is the Zn-bound thiolate, the S-VWN/6-31+G(d) method appears adequate for geometry optimization of the Zn complexes studied.

Validation of the Computed Relative Free Energies. To validate the methods used in computing the free energies, we

dx.doi.org/10.1021/ja202165x |J. Am. Chem. Soc. 2011, 133, 8691–8703

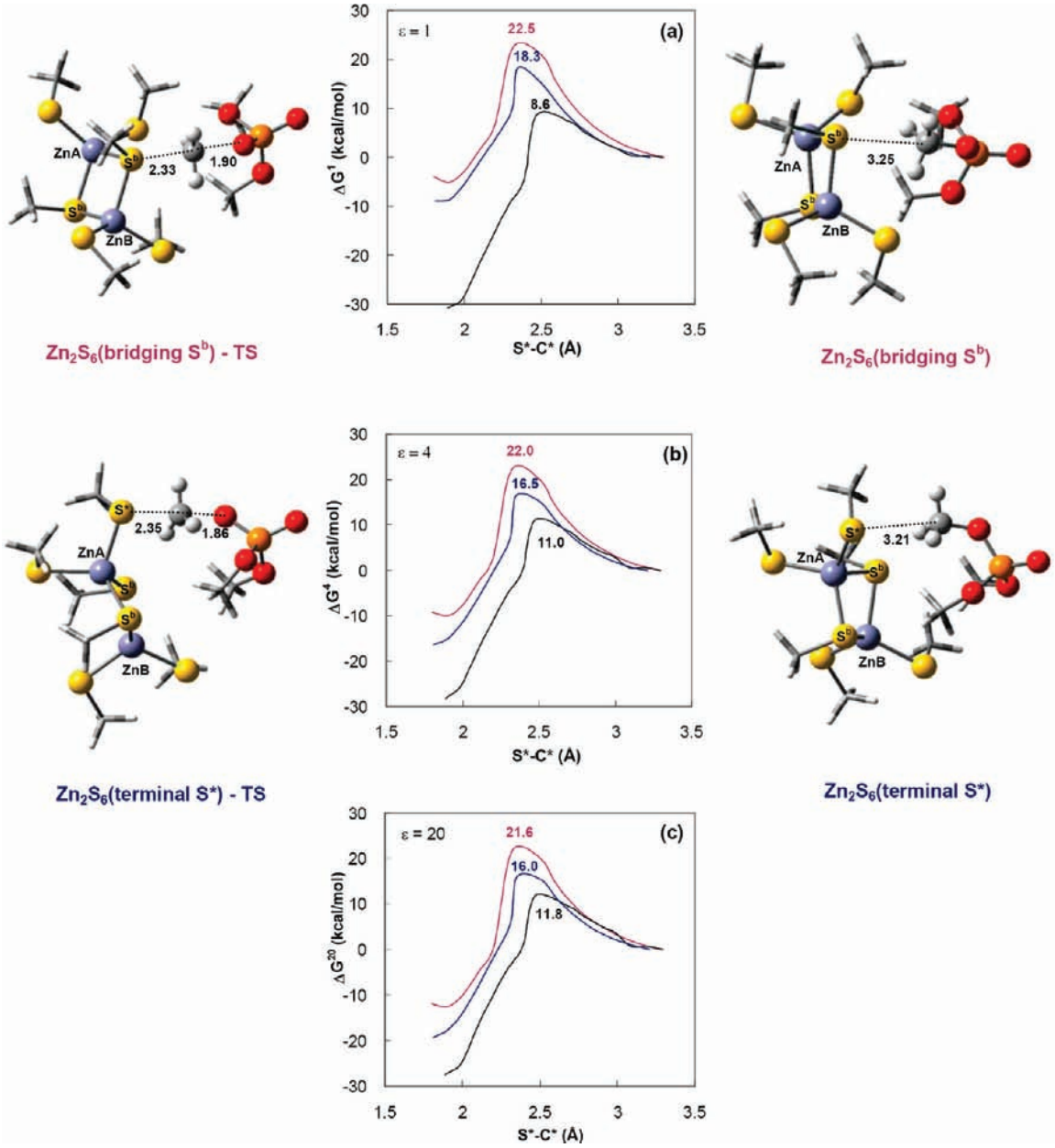

Figure 6. Free energy (in kcal/mol) as a function of the distance between the attacking S^b (maroon curves) or S* (blue curves) and the closest carbon of $(MeO)_3PO$ in the binuclear $[Zn_2(MeS)_6]^{2-}$ complex in (a) the gas phase ($\varepsilon = 1$), (b) buried sites ($\varepsilon = 4$), and (c) partially buried sites ($\varepsilon = 20$). These free energy profiles are compared to those in the mononuclear $[Zn(MeS)_4]^{2-}$ complex (black curves). The fully optimized S-VWN/6-31+G(d) geometries of the reactants and transition states are depicted on the right and left, respectively.

evaluated if the calculations could reproduce the trends in the methylation rates of model Zf cores, composed of benzenethiolate (SC_6H_5) and 1-methylimidazole (MeIm). The rate constants for reactions of these model Zf cores with $(MeO)_3PO$ in dimethyl sulfoxide (DMSO) solution decrease in the order $[Zn(SC_6H_5)_4]^{2-}$ > $[Zn(SC_6H_5)_3(MeIm)]^-$ ≫ $[Zn(SC_6H_5)_2(MeIm)_2]^0$.[21,36] Because the experimental results are consistent with a dissociated thiolate being the active species, we computed the free energy profiles for dissociation of a thiolate bound to $[Zn(SC_6H_5)_4]^{2-}$, $[Zn(SC_6H_5)_3(MeIm)]^-$, and $[Zn(SC_6H_5)_2(MeIm)_2]^0$ in the gas phase ($\varepsilon = 1$) and in DMSO ($\varepsilon = 47$). The computed free energies as a function of the distance between Zn and the departing S* in DMSO (Figure 2b) are consistent with the experimental methylation rates of these Zn complexes: the ΔG^{47} for pulling S* > 3 Å from Zn in $[Zn(SC_6H_5)_4]^{2-}$ (black curve) is less than that in $[Zn(SC_6H_5)_3(MeIm)]^-$ (red curve), which in turn is less than that in $[Zn(SC_6H_5)_2(MeIm)_2]^0$ (blue curve). As the thiolate dissociates, a DMSO molecule may bind to Zn, which would lower the free energy, but we did not map out the detailed mechanism of the dissociative pathway because our purpose here was to verify that the calculations could yield reliable trends in the free energies. Notably, the results below are based on relative (as opposed to absolute) free energies, where systematic errors would cancel to a large extent.

Effect of Zn Ligands on the Reactivity of an Unsheltered Cys. As the above results indicate that thiolate reactivity depends

dx.doi.org/10.1021/ja202165x |*J. Am. Chem. Soc.* 2011, 133, 8691–8703

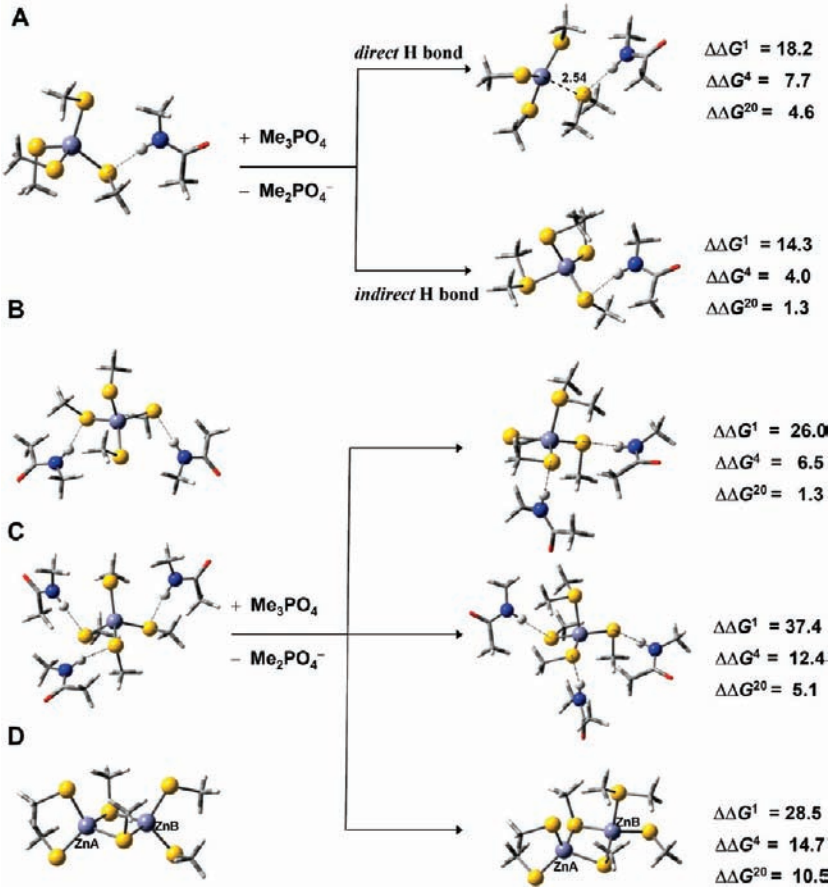

Figure 7. Effects of H bond(s) or dative bonds on the reaction free energies of $[Zn(MeS)_4]^{2-}$ complexes. (A) $[Zn(MeS)_4]^{2-}$ with a direct or an indirect backbone H bond, (B) $[Zn(MeS)_4]^{2-}$ with two backbone H bonds, (C) $[Zn(MeS)_4]^{2-}$ with three backbone H bonds, and (D) $[Zn_2(MeS)_6]^{2-}$, modeling a binuclear Zn_2Cys_6 site where the two Zn ions are denoted by ZnA and ZnB. The $\Delta\Delta G^x$ values (in kcal/mol) are relative to the methylation free energy of the isolated $[Zn(MeS)_4]^{2-}$ complex; that is, $[Zn(MeS)_4]^{2-} + Me_3PO_4 \rightarrow [Zn(MeS)_3(Me_2S)]^- + Me_2PO_4^-$, whose ΔG^1, ΔG^4, and ΔG^{20} values are −80.4, −33.6, and −21.1 kcal/mol, respectively. The fully optimized S-VWN/6-31+G(d) geometries of the reactant and product metal complexes are shown on the left and right, respectively.

on the Zn ligands, we evaluated the reactivity of an unprotected Cys in model Cys_4, Cys_3His, and Cys_2His_2 Zf cores via both dissociative and associative pathways. The free energy profiles for the dissociation or methylation of a Zn-bound thiolate in $[Zn(MeS)_4]^{2-}$, $[Zn(MeS)_3Im]^-$, and $[Zn(MeS)_2(Im)_2]$ complexes in the gas phase (ε = 1) and in fully/partially buried sites (ε = 4/20) were computed. The results for both dissociative and associative pathways show that the reactivity of an unprotected Cys in a fully or partially buried Zf core decreases with decreasing number of Cys ligands: the free energy for dissociation of a Zn-bound thiolate in Figure 3 increases in going from $[Zn(MeS)_4]^{2-}$ (black curve) to $[Zn(MeS)_3Im]^-$ (red curve) to $[Zn(MeS)_2(Im)_2]$ (blue curve). The increase in ΔG^x correlates with an increase in the Zn charge, whose NBO charge is 1.19e, 1.24e, and 1.32e in the isolated $[Zn(MeS)_4]^{2-}$, $[Zn(MeS)_3Im]^-$, and $[Zn(MeS)_2(Im)_2]^0$ complexes, respectively. In analogy to the dissociation free energy profiles, the free energy barrier for methylation of a Zn-bound thiolate in Figure 4 increases in going from $[Zn(MeS)_4]^{2-}$ (black curve) to $[Zn(MeS)_3Im]^-$ (violet and red curves) to $[Zn(MeS)_2(Im)_2]$ (blue curve). Notably, in the model Zn·Cys_3His core, the methylation barrier is lowered if the imidazole NH forms a H bond with a phosphate oxygen (compare red and violet curves in Figure 4).

Effect of Indirect H Bonds on the Zn·Cys_4 Reactivity. To determine if indirect H bonds to the Zn-bound cysteines can inhibit reaction at an unsheltered Cys (see Scheme 1), we evaluated the free energy barrier for transferring a methyl group from $(MeO)_3PO$ to a Zn-bound Cys of Cys_4 cores containing H bond(s) between the other cysteines and the peptide backbone. The corresponding free energy barrier for a Zn-bound thiolate H-bonded directly to $CH_3CONHCH_3$ was also calculated to compare the effect of a direct H bond with that of an indirect one. Figure 5 shows the resulting free energy profiles for Cys_4 cores containing no H bonds (black curves), one direct H bond (gray curves), one indirect H bond (green curves), two indirect H bonds (blue curves), and three indirect H bonds (orange curves) to the peptide backbone in the gas phase and in fully/partially buried sites; the fully optimized reactant structures are depicted on the right, whereas the corresponding TS structures are shown on the left. These free energy profiles show that, although a single indirect NH---S hydrogen bond does not appear to protect the Zn-bound thiolate, two or more indirect NH---S hydrogen bonds offer more protection than a direct backbone H bond. For example, in a buried site (ε = 4), three indirect backbone H bonds raise the free energy barrier for methylation of a Zn-bound thiolate in an isolated Cys_4 core by 6.9 kcal/mol (from 11.0 to

dx.doi.org/10.1021/ja202165x | J. Am. Chem. Soc. 2011, 133, 8691–8703

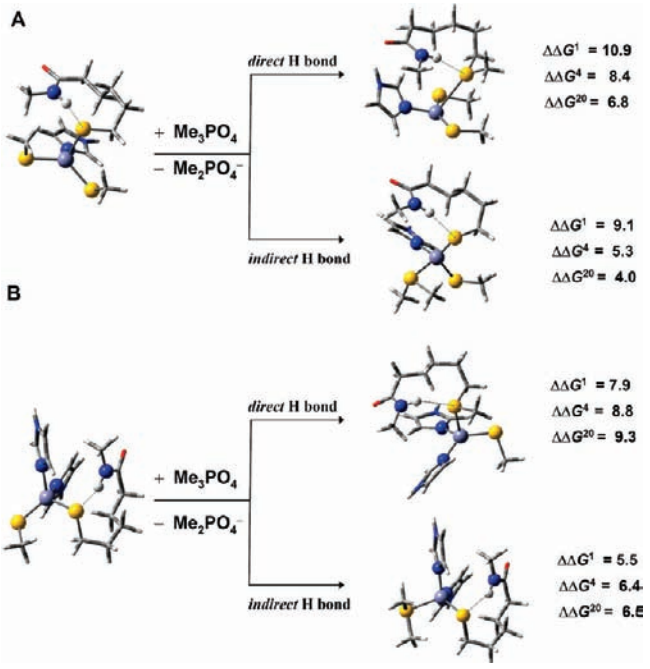

Figure 8. Effects of H-bond interactions on the reaction free energies of $[Zn(MeS)_3(Im)]^-$ and $[Zn(MeS)_2(Im)_2]^0$ complexes. (A) $[Zn(MeS)_3(Im)]^-$ with a direct or an indirect backbone H bond. The $\Delta\Delta G^x$ values (in kcal/mol) are relative to the free energy for $[Zn(MeS)_3(Im)]^- + Me_3PO_4 \rightarrow [Zn(MeS)_2(Im)(Me_2S)]^0 + Me_2PO_4^-$, whose ΔG^1, ΔG^4, and ΔG^{20} values are −6.3, −17.5, and −20.5 kcal/mol, respectively. (B) $[Zn(MeS)_2(Im)_2]^0$ with a direct or an indirect backbone H bond. The $\Delta\Delta G^x$ values (in kcal/mol) are relative to the free energy for $[Zn(MeS)_2(Im)_2]^0 + Me_3PO_4 \rightarrow [Zn(MeS)(Im)_2(Me_2S)]^+ + Me_2PO_4^-$, whose ΔG^1, ΔG^4, and ΔG^{20} values are 69.2, 4.8, and −13.0 kcal/mol, respectively. The fully optimized S-VWN/6-31+G(d) geometries of the reactant and product metal complexes are shown on the left and right, respectively.

17.9 kcal/mol), whereas a direct backbone H bond raises it by only 1.9 kcal/mol (from 11.0 to 12.9 kcal/mol).

Effect of Metal−Ligand Bonds on the Zn·Cys$_4$ Reactivity. A Zn^{2+} in a polynuclear Zn-site coordinated to bridging cysteines can be considered to contribute direct bonds for the bridging S^b atoms and indirect bonds for the terminal S* atoms. For example, the second Zn (denoted as ZnB) in the binuclear Zn_2Cys_6 site coordinates to two cysteines bridging the two Zn ions, thus contributing direct bonds for the bridging S^b atoms and two indirect bonds for the unprotected ZnA-bound S* atoms. To evaluate the effects of ZnB on the reactivity of ZnA-bound Cys, the free energy profiles for the methylation of a bridging S^b and a ZnA-bound S* in $[Zn_2(MeS)_6]^{2-}$ were computed. The results in Figure 6 indicate that bonds from ZnB to the bridging cysteines inhibit the bridging S^b reactivity (maroon curves) more than the terminal S* reactivity (blue curves). For example, in a buried site ($\varepsilon = 4$), the direct bonds from ZnB to the bridging S^b atoms raise the free energy barrier for methylation of S^b from 11 kcal/mol in $[Zn(MeS)_4]^{2-}$ to 22 kcal/mol in $[Zn_2(MeS)_6]^{2-}$. Because the second Zn forms direct bonds with the bridging S^b atoms, but provides indirect bonds for the unprotected ZnA-bound S* atoms, the methylation free energy barrier of a terminal ZnA-bound S* in the $[Zn_2(MeS)_6]^{2-}$ complex (16.5 kcal/mol) is lower than that of a bridging S^b (by 5.5 kcal/mol), but still higher than that in the isolated $[Zn(MeS)_4]^{2-}$ complex (by 5.5 kcal/mol).

Effects of Indirect Bonds on the Zn·Cys$_4$ Stability. To determine if indirect H bonds or metal−ligand bonds to Zn-bound cysteines can not only inhibit reaction at an unsheltered Cys, but also stabilize the Zf core, we computed the $\Delta\Delta G^x$ free energies for methylation of a Zn-bound thiolate in (i) $[Zn(MeS)_4]^{2-}$ containing one or more NH---S hydrogen bonds, and (ii) $[Zn(MeS)_4 \cdot Zn(MeS)_2]^{2-}$ relative to those in the isolated complex. The positive $\Delta\Delta G^x$ values in Figure 7 indicate that indirect H bonds or metal−ligand bonds can help to stabilize a buried Zn·Cys$_4$ core. Increasing the number of indirect NH---S hydrogen bonds increases the stability of the Zf core such that three indirect NH---S hydrogen bonds could stabilize the Zf core more than a direct one: the relative methylation $\Delta\Delta G^4$ free energy of an unshielded thiolate in a buried $[Zn(MeS)_4]^{2-}$ site containing three NH---S hydrogen bonds (12.4 kcal/mol, Figure 7C) is greater than that of a shielded thiolate (7.7 kcal/mol, Figure 7A). Furthermore, a binuclear Zn_2Cys_6 core is more stable than a mononuclear Zn·Cys$_4$ core. Interestingly, the gas-phase $\Delta\Delta G^1$ for the $[Zn(MeS)_4 \cdot Zn(MeS)_2]^{2-}$ core (28.5 kcal/mol, Figure 7D) is similar to that for the $[Zn(MeS)_4 \cdot (MeCONHMe)_2]^{2-}$ core (~26.0 kcal/mol, Figure 7B). The former is stabilized by two bonds from neutral $[ZnB(MeS)_2]$, while the latter is stabilized by two indirect H bonds from the neutral backbone peptide. Thus, the second Zn in a binuclear Zn_2Cys_6 core can be considered to contribute indirect bonds, which helps to stabilize the Zn site.

Effects of Indirect Bonds on the Zn·Cys$_3$His and Zn·Cys$_2$His$_2$ Stability. To assess if indirect H bonds can also help to stabilize Cys$_3$His and Cys$_2$His$_2$ Zf cores of varying solvent exposure, we computed the free energies for methylation of a Zn-bound thiolate in the $[Zn(MeS)_3Im]^-$ and $[Zn(MeS)_2(Im)_2]$ complex containing a direct/indirect NH---S hydrogen bond relative to those in the respective isolated complex. The positive $\Delta\Delta G^x$ values in Figure 8 indicate that both direct and indirect H bonds can help to stabilize a Zn·Cys$_3$His or Zn·Cys$_2$His$_2$ core. In a buried site ($\varepsilon = 4$), a single direct NH---S hydrogen bond stabilizes the Cys$_3$His or Cys$_2$His$_2$ core by 8−9 kcal/mol, whereas an indirect one stabilizes the respective Zf core by 5−6 kcal/mol.

Physical Basis for the Effects of Indirect Bonds on Thiolate Reactivity. To elucidate why indirect H bonds inhibit reaction at the other unsheltered ligands in Zn·Cys$_4$ cores, we computed the NBO[52] atomic charges of Cys$_4$ cores containing 0, 1, 2, and 3 NH---S hydrogen bonds. Comparison of the atomic charges of Cys$_4$ cores with backbone hydrogen bonds with those in the isolated complex shows that the indirect H bonds reduce the atomic charge of an unshielded Cys S^- and thus its nucleophilicity through withdrawal of its charge to the more electronegative backbone carbonyl O. For example, relative to the NBO charges of the isolated $[Zn(MeS)_4]^{2-}$ complex, the largest change in the NBO charges of the $[Zn(MeS)_4]^{2-}$ complex containing three indirect backbone H bonds occurs at the carbonyl O atoms, whose charges are increased by ~12%. On the other hand, the charges on the three shielded S^- atoms are reduced by ~10%, whereas the charge on the unshielded S^- is reduced by 8% (see Figure 9A). Interestingly, the gas-phase ΔG^1 free energy barriers for the methylation of an unshielded Zn-bound thiolate in a Cys$_4$ core containing 0, 1, 2, or 3 indirect H bonds (from Figure 5a) correlate with the mean NBO charge on the unshielded S, as evidenced by a Pearson correlation coefficient $r^2 = 0.949$ (see Figure 9B).

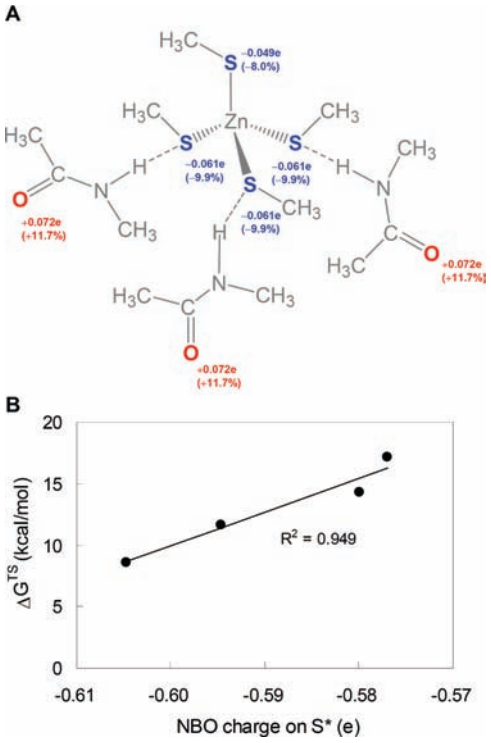

Figure 9. (A) NBO charge analysis of $[Zn(MeS)_4]^{2-}$ with three backbone H bonds. Those NBO charges that exhibit the largest increase and decrease relative to the isolated $[Zn(MeS)_4]^{2-}$ complex are shown in red and blue, respectively. (B) Correlation between the gas-phase ΔG^1 free energy barriers for the methylation of an unshielded Zn-bound S* in a Cys_4 core containing 0, 1, 2, or 3 indirect NH---S hydrogen bonds (from Figure 5a) and the mean NBO charge on the reacting S*. The Pearson correlation coefficient is 0.949.

DISCUSSION

Factors Controlling Zf Reactivity. The above results in conjunction with results from previous studies reveal the key factors suppressing the Zn-bound thiolate reactivity in a Zf core and the physical basis for the observed trends. Below, we list these factors in order of the number and strength of the interactions with the reacting S*. Notably, the calculations support our hypothesis that unsheltered Cys ligands may be protected by indirect bonds to other Cys ligands (see Introduction).

i. Direct H Bonds. In accord with previous studies on model Zf cores,[53] a Zn-bound S* will become less reactive if it is directly H-bonded to the peptide backbone or other residues in the second shell (Figure 5, compare gray and black curves). This is because a Zn-bound S* becomes less nucleophilic when it forms H bond(s): the NBO charge on a Zn-bound S* H-bonded to $CH_3CONHCH_3$ (−0.54e) is less negative than that in the isolated $[Zn(MeS)_4]^{2-}$ complex (∼ −0.62e).

ii. Indirect Bonds from Zn Ligands. The reactive thiolate S* is connected to the other Zn ligand (L) atoms via two bonds: S*−Zn and Zn−L. Because a negatively charged Cys^- transfers more charge to Zn than a neutral His,[9] the net charge transfer from the ligands to Zn decreases, while the positive charge on the Zn increases, in the order Cys_4 > Cys_3His > Cys_2His_2. Notably, the gas-phase ΔG^1 free energy barriers for the methylation of an unshielded Zn-bound thiolate in Cys_4, Cys_3His, and Cys_2His_2 Zf cores (from Figure 4a) exhibit a linear correlation with the NBO charge on Zn, as evidenced by a Pearson correlation coefficient, $r^2 \approx 0.994$. A higher positive charge on Zn inhibits methylation/dissociation of the negatively charged thiolate; hence the increase in the Zn charge with increasing number of His ligands in the Zf cores correlates with the decrease in reactivity of these cores (see Figures 3 and 4). This finding is consistent with the empirical findings that (i) neutral Zf cores are inherently more resistant to alkylation reactions than anionic cores,[15,21] and (ii) the number of backbone NH---S hydrogen bonds per Zf core decreases from 6.4 for Cys_4 to 4.0 for Cys_3His to 2.5 for Cys_2His_2.[25]

iii. Indirect Bonds from a Second Zn Site. The reactive thiolate S* is connected to the second ZnB in a binuclear Zn_2Cys_6 core via three bonds: S*−ZnA, ZnA−S^b, and S^b−ZnB (Figure 6). The mean NBO charge on the bridging S^b (−0.57e) or unsheltered S* (−0.58e) in the binuclear Zn_2Cys_6 core is less than that on the S atoms in the mononuclear Zn·Cys_4 complex (−0.62e). Hence, the reactivity of the S^b or S* atom is suppressed and the binuclear Zn_2Cys_6 core is stabilized relative to the mononuclear Zn·Cys_4 core with the same net charge. This finding provides a rationale why some polynuclear Zf cores exhibit a lack of H−bond protection (see Table 1),[25] but are not known to be reactive.

iv. Indirect H Bonds. The reactive thiolate S* is connected to the H-bond donor participating in an indirect H bond with a Zn-bound Cys via two bonds and a H bond: S*−Zn, Zn−S, S---H(N). In analogy to the second Zn in a binuclear Zn_2Cys_6 core, the presence of indirect H bonds to the Zn-bound thiolates results in a reduced charge on the unsheltered S*: the mean S* NBO charge in the model Cys_4 core containing one (−0.60e), two (−0.59e), and three (−0.57e) H bonds with the backbone amide is less than that in the isolated Zn·Cys_4 complex (−0.62e), as the negative charge is withdrawn to the more electronegative backbone carbonyl O. Notably, three indirect NH---S hydrogen bonds could offer more protection than a single direct one (Figure 5, compare orange and

dx.doi.org/10.1021/ja202165x |J. Am. Chem. Soc. 2011, 133, 8691–8703

gray curves). In contrast to NH---S hydrogen bonds, a NH---O hydrogen bond between the imidazole NH and a phosphate O could enhance reactivity of S* (Figure 4, compare violet and red curves).

v. Solvent Exposure of the Zf Core. Denying solvent access to a Cys_2His_2 Zf core stabilizes it, as the reaction, $[Zn(MeS)_2(Im)_2]^0 + Me_3PO_4 \rightarrow [Zn(MeS)(Im)_2(Me_2S)]^+ + Me_2PO_4^-$, is thermodynamically unfavorable in a buried site (positive ΔG^x, $x \leq 4$, Figure 8 footnote). This is consistent with the fact that structural Cys_2His_2 sites are found to be buried in a PDB survey.[25] However, the reaction becomes favorable when the site becomes solvent exposed, due mainly to the favorable solvation of the charged products as compared to the neutral reactants. On the other hand, partial solvent exposure of the Zf core does not significantly affect the protective effects of both direct and indirect H bonds. The free energy barriers for methylation of a Zn-bound S in a fully or partially buried Cys_4 core differ by <1 kcal/mol (Figure 5, compare ΔG^4 and ΔG^{20}).

Biological Implications. The results herein help to elucidate why Zf cores with unsheltered Cys ligands are not known to be reactive (Table 1). Indirect H bonds can stabilize such structural cores. For example, the Zn·Cys_4 core in human PARP-1 (2jvn) and the Zn·Cys_3His core in tRNA-guanine transglycosylase (1pud) each has two H-bonded cysteines. Although the Zn·Cys_2His_2 cores of Zif268 (1aay) and endoglucanase (1clc) lack H-bond protection, their inaccessibility to solvent and the reduced charge transfer from the histidines to Zn help protect these cores.

The results also help to elucidate guidelines for distinguishing labile Cys-rich Zn sites from structural ones: labile Cys-rich Zn sites are likely to be buried Cys_4 cores or solvent-exposed Cys_3His cores containing unsheltered cysteines. Indeed, the known labile Cys_4 and Cys_3His Zf cores in human/chicken estrogen receptor (1hcp), *E. coli* N-Ada (1eyf), FOG-1 (1fu9), MMTV nucleocapsid protein (1dsq), HIV-1 nucleocapsid protein (2exf), and histone demethylase JMJD2A (2oq6) contain no cysteines with H-bonding interactions (Table 1). Notably, the labile Zn·Cys_3His cores in the HIV-1 nucleocapsid protein and histone demethylase JMJD2A, a potential anticancer drug target,[54] can react with Zn-ejecting reagents.[55]

Any changes in the interactions and solvent exposure of the Cys-rich Zn site upon substrate binding would impact on the Zn-bound thiolate reactivity. This is supported by the finding that the Zn·Cys_4 core of free N-Ada (1eyf) has no H bonds to second-shell residues and is found to be reactive, whereas the DNA-bound form of N-Ada (1u8b) exhibits several H-bonding interactions and is found to be inactive. The selective methylation of Cys38 in N-Ada may be due to its proximity to the methyl group on DNA: the distances from the Cys38, Cys42, Cys69, and Cys72 S atoms to the methylated DNA P atom in the 1u8b X-ray structure are 4.9, 7.2, 6.6, and 8.6 Å, respectively.

■ ASSOCIATED CONTENT

Supporting Information. Complete refs 31 and 44 and Supplementary Tables S1 and S2. This material is available free of charge via the Internet at http://pubs.acs.org.

■ AUTHOR INFORMATION

Corresponding Author
carmay@gate.sinica.edu.tw

■ ACKNOWLEDGMENT

We thank Dr. Todor Dudev for helpful discussions. This work is supported by the Institute of Biomedical Sciences, Academia Sinica and by NSC contract no. NSC 95-2113-M-001-001.

■ REFERENCES

(1) Vallee, B. L.; Auld, D. S. *Proc. Natl. Acad. Sci. U.S.A.* **1990**, *87*, 220.
(2) Coleman, J. E. *Annu. Rev. Biochem.* **1992**, *61*, 897.
(3) Lipscomb, W. N.; Sträter, N. *Chem. Rev.* **1996**, *96*, 2375.
(4) Berg, J. M.; Godwin, H. A. *Annu. Rev. Biophys. Biomol. Struct.* **1997**, *26*, 357.
(5) Dudev, T.; Lim, C. *J. Am. Chem. Soc.* **2002**, *124*, 6759.
(6) Maret, W. *Antioxid. Redox Signaling* **2006**, *8*, 1419.
(7) Maret, W.; Li, Y. *Chem. Rev.* **2009**, *109*, 4682.
(8) Sri Krishna, S.; I., M.; Grishin, N. V. *Nucleic Acids Res.* **2003**, *31*, 532.
(9) Lee, Y.-M.; Lim, C. *J. Mol. Biol.* **2008**, *379*, 545.
(10) Garmer, D. R.; Gresh, N. *J. Am. Chem. Soc.* **1994**, *116*, 3556.
(11) Dudev, T.; Lim, C. *J. Phys. Chem. B* **2001**, *105*, 4446.
(12) Quintal, S. M.; dePaula, Q. A.; Farrell, N. P. *Metallomics* **2011**, *3*, 121.
(13) Rice, W. G.; Schaeffer, C. A.; Harten, B.; Villinger, F.; South, T. L.; Summers, M. F.; Henderson, L. E.; Bess, J. W.; Arthur, L. O.; McDougal, J. S.; Orloff, S. L.; Mendeleyev, J.; Kun, E. *Nature* **1993**, *361*, 473.
(14) Loo, J. A.; Holler, T. P.; Sanchez, J.; Gogliotti, R.; Maloney, L.; Reily, M. D. *J. Med. Chem.* **1996**, *39*, 4313.
(15) Miller-Jenkins, L. M. M.; Durell, S. R.; Maynard, A. T.; Stahl, S. J.; Inman, J. K.; Appella, E.; Legault, P.; Omichinski, J. G. *J. Am. Chem. Soc.* **2006**, *128*, 11964.
(16) Miller-Jenkins, L. M.; Hara, T.; Durell, S. R.; Hayashi, R.; Inman, J. K.; Piquemal, J.-P.; Gresh, N.; Appella, E. *J. Am. Chem. Soc.* **2007**, *129*, 11067.
(17) Huang, M.; Maynard, A.; Turpin, J. A.; Graham, L.; Janini, G. M.; Covell, D. G.; Rice, W. G. *J. Med. Chem.* **1998**, *41*, 1371.
(18) Wang, L. H.; Yang, X. Y.; Zhang, X.; Mihalic, K.; Fan, Y.-X.; Xiao, W.; Howard, O. M. Z.; Appella, E.; Maynard, A. T.; Farrar, W. L. *Nat. Med.* **2004**, *10*, 40.
(19) Wang, L. H.; Yang, X. Y.; Zhang, X.; An, P.; Kim, H.-J.; Huang, J.; Clarke, R.; Osborne, C. K.; Inman, J. K.; Appella, E.; Farrar, W. L. *Cancer Cell* **2006**, *10*, 487.
(20) He, C.; Hus, J.-C.; Sun, L. J.; Zhou, P.; Norman, D. P. G.; Dötsch, V.; Wei, H.; Gross, J. D.; Lane, W. S.; Wagner, G.; Verdine, G. L. *Mol. Cell* **2005**, *20*, 117.
(21) Wilker, J. J.; Lippard, S. J. *Inorg. Chem.* **1997**, *36*, 969.
(22) Warthen, C. R.; Hammes, B. S.; Carrano, C. J.; Crans, D. C. *J. Biol. Inorg. Chem.* **2001**, *6*, 82.
(23) Picot, D.; Ohanessian, G.; Frison, G. *Inorg. Chem.* **2008**, *47*, 8167.
(24) Picot, D.; Ohanessian, G.; Frison, G. *Chem. Asian J.* **2010**, *5*, 1445.
(25) Maynard, A. T.; Covell, D. G. *J. Am. Chem. Soc.* **2001**, *123*, 1047.
(26) Chiou, S.-J.; Riordan, C. G.; Rheingold, A. L. *Proc. Natl. Acad. Sci. U.S.A.* **2003**, *100*, 3695.
(27) Smith, J. N.; Shirin, Z.; Carrano, C. J. *J. Am. Chem. Soc.* **2003**, *125*, 868.
(28) Parkin, G. *Chem. Rev.* **2004**, *104*, 699.
(29) Myers, L. C.; Verdine, G. L.; Wagner, G. *Biochemistry* **1993**, *32*, 14089.
(30) Mishina, Y.; Duguid, E.; He, C. *Chem. Rev.* **2006**, *106*, 215.
(31) Berman, H. M.; et al. *Acta Crystallogr., Sect. D* **2002**, *58*, 899.
(32) McDonald, I. K.; Thornton, J. M. *J. Mol. Biol.* **1994**, *238*, 777.
(33) Hubbard, S. J.; Thornton, J. M. Department of Biochemistry and Molecular Biology, University College: London, 1993.
(34) Penner-Hahn, J. *Curr. Opin. Chem. Biol.* **2007**, *11*, 166.

(35) Lipton, A. S.; Ellis, P. D. *J. Am. Chem. Soc.* **2007**, *129*, 9192.
(36) Wilker, J. J.; Lippard, S. J. *J. Am. Chem. Soc.* **1995**, *117*, 8682.
(37) Morlok, M. M.; Janak, K. E.; Zhu, G.; Quarless, D. A.; Parkin, G. *J. Am. Chem. Soc.* **2005**, *127*, 14039.
(38) Gockel, P.; Gelinsky, M.; Vogler, R.; Vahrenkamp, H. *Inorg. Chim. Acta* **1998**, *272*, 115.
(39) Bridgewater, B. M.; Fillebeen, T.; Friesner, R. A.; Parkin, G. *J. Chem. Soc., Dalton Trans.* **2000**, 4494.
(40) Dudev, T.; Lin, Y. L.; Dudev, M.; Lim, C. *J. Am. Chem. Soc.* **2003**, *125*, 3168.
(41) Lin, Y.-l.; Lim, C. *J. Am. Chem. Soc.* **2004**, *126*, 2602.
(42) Lin, Y.-l.; Lee, Y.-M.; Lim, C. *J. Am. Chem. Soc.* **2005**, *127*, 11336.
(43) Dudev, T.; Lim, C. *J. Am. Chem. Soc.* **2006**, *128*, 1553.
(44) Frisch, M. J.; et al. Gaussian, Inc.: Pittsburgh, PA, 2003.
(45) Dudev, T.; Lim, C. *J. Am. Chem. Soc.* **2007**, *129*, 12497.
(46) Wong, M. W. *Chem. Phys. Lett.* **1996**, *256*, 391.
(47) McQuarrie, D. A. *Statistical Mechanics*; Harper and Row: New York, 1976.
(48) Bashford, D. In *Scientific Computing in Object-Oriented Parallel Environments*; Ishikawa, Y., Oldehoeft, R. R., Reynders, V. W., Tholburn, M., Eds.; Springer: Berlin, 1997; Vol. 1343, p 233.
(49) Chan, S. L.; Lim, C. *J. Phys. Chem.* **1994**, *98*, 692.
(50) Brooks, B. R.; Bruccoleri, R. E.; Olafson, B. D.; States, D. J.; Swaminathan, S.; Karplus, M. *J. Comput. Chem.* **1983**, *4*, 187.
(51) Allen, F. H. *Acta Crystallogr.* **2002**, *B58*, 380.
(52) Reed, A.; Weinstock, R.; Weinhold, F. *J. Chem. Phys.* **1985**, *83*, 735.
(53) Konrat, R.; Weiskirchen, R.; Bister, K.; Kräutler, B. *J. Am. Chem. Soc.* **1998**, *120*, 7127.
(54) Cloos, P. A. C.; Christensen, J.; Agger, K.; Maiolica, A.; Rappsilber, J.; Antal, T.; Hansen, K. H.; Helin, K. *Nature* **2006**, *442*, 307.
(55) Sekirnik, R.; Rose, N. R.; Thalhammer, A.; Seden, P. T.; Mecinovic, J.; Schofield, C. J. *Chem. Commun.* **2009**, 6376.